

Evaluation of Track Following Servo Performance for Patterned Servo Sectors in Hard Disk Drives

Younghee Han and Raymond A. de Callafon

University of California at San Diego, Mechanical and Aerospace Engineering
9500 Gilman Drive, La Jolla, CA, 92093-0401, USA

Abstract—A promising approach for ultra high data storage capacities in magnetic hard disk drives is the use of bit-patterned media (BPM) that allows both higher track densities and increased linear bit spacing of data. To allow for such ultra high track densities, it is important to select an embedded servo pattern within the BPM that provides a Position Error Signal (PES) with sufficient quality to maintain (high bandwidth) head positioning. This paper discusses servo pattern performance from a closed-loop point of view for several servo patterns that could be incorporated in a BPM. A dedicated magnetic readback signal simulation and signal decoding along with a closed-loop simulation are used to evaluate tracking and PES quality. Due to PES nonlinearity in the conventional amplitude based servo pattern currently used in most drives, a timing based chevron pattern and a differential frequency pattern are considered as case studies in this paper. For the timing based servo patterns, both readback signal sampling and transition jitter were found to greatly affect PES quality. It is shown by the simulation studies in this paper that the differential frequency servo pattern can surpass the chevron and amplitude based servo patterns when subjected to sampling and jitter noise due to the averaging effects of the rotational symmetry of the pattern.

I. INTRODUCTION

To achieve thermal stability in ultra-high density magnetic recording, the use of bit patterned media (BPM) has been proposed as a possible solution for future hard disk drive (HDD) development. The main idea for thermal stability in BPM comes from creating predefined magnetic islands providing isolated signal domains in which each bit is stored [1], [2]. Data densities in excess of 10Tbit/in², BPM with magnetic islands in the order of 10nm² at 10nm spacing provide a challenge for both media manufacturing, head read/write design, flying height constraints and servo design. This paper focuses on the servo related aspects, and in particular the quality of the Position Error Signal (PES) used for the servo system to maintain data tracking when using different embedded servo patterns in the BPM.

As the PES used in HDD servo control is obtained by demodulating readback signals from embedded servo patterns on the HDD, the quality of the PES in conventional media noise is influenced by media noise and readback signal properties [3], [4]. In addition, the PES can exhibit non-linearities due to the inherent non-linear response of (G)MR heads [5]. Next to these effects, PES quality can be severely impacted due to misalignment of the actual servo burst patterns recorded and embedded between the data in the servo sectors on a HDD [6]. Obviously, most of these

effects may still be present when designing servo patterns in a BPM, but the possible design freedom that exists in a BPM can be used to use a servo pattern where the PES is less susceptible to these influences.

Motivated by the favorable properties of BPM, there is a growing body of literature on BPM recording and performance evaluation of servo patterns. Basic recording physics, characteristics and advantages of a BPM recording can be found in [7], [8], [9], [10], [11]. Previous studies that compare PES performance of different servo patterns for HDDs using BPM has been conducted in [12], [13], [14]. These contributions illustrate that patterned servo bits provide excellent PES recovery and that more advanced servo patterns should be used to improve PES quality and servo performance. This paper builds on these results by evaluating the quality of the PES generated by several different servo patterns from a closed-loop (servo) point of view.

In this paper PES quality is evaluated by a dedicated magnetic readback signal simulation and signal decoding along with a closed-loop simulation based on models and controllers from existing benchmark problem [15]. The PES quality is characterized by important quality factors that are known to affect PES quality: amplitude fluctuation noise, transition jitter, signal sampling and timing jitter. The procedure outlined in this paper is applicable to any servo pattern but the attention is focused on the comparison of a conventional amplitude-based pattern with two new timing-based patterns (chevron pattern, and differential frequency pattern, see [16]) as case studies to evaluate PES quality. For the timing based servo patterns, both readback signal sampling and transition jitter will greatly affect PES quality. However, the rotational symmetry of the differential frequency servo pattern will prove to be beneficial in providing averaging of signal sampling and transition jitter effects.

II. SIMULATION OF READBACK SIGNALS

A. Readback signal generation

PES is obtained by demodulating a readback signal $R(t)$ obtained by measuring the magnetic orientation of a servo pattern embedded in between the data on a HDD. To compute a readback signal $R(t)$ from a servo pattern, two signals are used. In general, a readback signal $R(t)$ is calculated by the convolution of a transition response $h(t, w)$ and a bit pattern signal $b(t)$ determined by the actual servo patterns. Following

[17] a readback signal $R(t)$ is modeled as a convolution

$$R(t) = \int h(t, w) \cdot \frac{d}{dt} b(t - \tau) d\tau$$

where $\frac{d}{dt} b(t - \tau)$ indicates the derivative of a bit pattern signal $b(t)$ due to the magnetic orientation. For longitudinal recording, a transition response $h(t, w)$ is modeled as the Lorentzian pulse.

$$h(t, w) = \frac{V_p}{1 + (\frac{2t}{w})^2}$$

where V_p is the peak value of the $h(t, w)$ and w is the width of $h(t, w)$ at half of its peak value. For perpendicular media, a transition response $h(t, w)$ can be modeled as [17]:

$$h(t, w) = V_p \cdot \operatorname{erf}\left(\frac{2\sqrt{\ln 2}}{w} t\right)$$

where $\operatorname{erf}(x)$ is the error function, defined as:

$$\operatorname{erf}(t) = \frac{2}{\sqrt{\pi}} \int_0^t e^{-x^2} dx$$

To model the effect of different servo patterns and to be able to incorporate amplitude fluctuation noise, the bit pattern signal $b(t)$ will be oversampled in the simulation. The oversampling allows additional signals to be added to the pattern signal $b(t)$, providing a unique way to incorporate (spatial) uncertainty and (media) noise into the readback signal $R(t)$. Using the notation $b(k)$ to indicate an oversampled bit pattern signal $b(k\Delta T)$ and a discrete-time convolution, we write a readback signal $R(k)$ via

$$R(k) = \sum_j h_{\Delta T}(j, w) \cdot [(b(k - j) - b(k - 1 - j))]$$

where $h_{\Delta T}(k, w)$ indicates the sampled transition response $h_{\Delta T}(k, w) = \frac{1}{\Delta T} \cdot h(k\Delta T, w)$.

Hence, once a servo pattern is designed and repeated along the servo sectors of the HDD, a readback signal $R(k)$ can be generated from the patterns. The oversampling of the bit pattern signal during the simulation allows noise on the bit pattern signal $b(k)$ to account for amplitude fluctuation noise and transition jitter effects can be handled by modulating the time shift in a transition response $h(k, w)$. This approach allows one to examine the quality of the readback signal and thus the resulting PES for a particular servo pattern.

B. Quality measures for readback signals

In this paper, two sources of media noise are considered: The amplitude fluctuation noise and the transition jitter [3], [4]. Amplitude fluctuation noise is amplitude fluctuation on a bit pattern signal $b(k)$ due to magnetic non-uniformities of the media. Various reasons, such as demagnetization field, media overwrite, adjacent track erasure (ATE), return-induced partial erase (RFPE), thermal fluctuation, etc., can affect amplitude fluctuation noise.

Using the notation $\aleph(\mu, \lambda)$ to indicate a normal distribution with a mean value μ and a variance λ , the amplitude fluctuation noise $\eta(k)$ are modeled as independent and identically

distributed (IID) samples from $\aleph(0, \lambda_\eta)$. Therefore, the bit pattern signal corrupted by amplitude fluctuation noise $\tilde{b}(k)$ is defined as $\tilde{b}(k) = b(k) + \eta(k)$, where $\eta(k) \sim \aleph(0, \lambda_\eta)$ and λ_η is the variance of amplitude fluctuation noise distribution. Therefore, the amplitude fluctuation noise effect on the readback signal $R(k)$ is modeled as

$$\begin{aligned} \tilde{b}(k) &= b(k) + \eta(k), \quad \eta(k) \sim \aleph(0, \lambda_\eta) \\ R(k) &= \sum_j h_{\Delta T}(j, w) [\tilde{b}(k - j) - \tilde{b}(k - 1 - j)] \end{aligned} \quad (1)$$

Servo burst patterns contain the sequence of magnetic transitions. Random magnetization fluctuations in transition positions cause phase shift in a bit pattern signal $b(k)$. This random signal phase shift due to random transition position fluctuations is called transition jitter, see e.g. [3], [4], [17]. In the simulation study presented in this paper, transition jitter effect are considered as time shifts in a transition response $h(k, w)$. Using the notation $\aleph(\mu, \lambda)$ as described earlier, the effect of transition jitter γ on a readback signal $R(k)$ is represented as

$$\begin{aligned} \tilde{h}_{\Delta T}(k, w) &= h_{\Delta T}(\kappa, w) \\ \kappa &= k + \gamma, \quad \gamma \sim \aleph(0, \lambda_\gamma) \\ R(k) &= \sum_j \tilde{h}_{\Delta T}(j, w) [\tilde{b}(k - j) - \tilde{b}(k - 1 - j)] \end{aligned} \quad (2)$$

and modeled as IID samples from $\aleph(0, \lambda_\gamma)$ on a time shifted $\tilde{h}_{\Delta T}(k, w) = h_{\Delta T}(\kappa, w)$, $\kappa = k + \gamma$ transition response.

In the digital domain, readback signal sampling is another important quality factor in the evaluation of readback signal quality. The readback signal sampling interval ΔT is determined by how many samples are used to sample a bit pattern signal $b(k)$. Given total time T_p spent reading the bit pattern signal $b(k)$, the readback signal sampling interval ΔT is given by

$$\Delta T = \frac{T_p}{N_p} \quad (3)$$

where N_p is the number of samples. The readback signal sampling effect on PES will be investigated by changing the number of samples N_p . These quality factors (amplitude fluctuation noise, transition jitter and signal sampling) will be used to evaluate the quality of the readback signal $R(k)$ and PES from different servo patterns (the servo patterns performance). Detailed simulation results of these effects will be presented in Section IV.

III. CLOSED-LOOP PES EVALUATION

A. Servo patterns and demodulation

The PES sampling interval $\Delta\tau$ is determined by the location of the servo sectors and the rotational speed of the HDD. For the analysis of PES quality, it can be assumed that the actuator stays on a same track during track following mode. Since PES is obtained at the same servo sectors repeatedly as the disk rotates, the sampling time can be written as

$$t = (m + kN) \cdot \Delta\tau, \quad m = 1, \dots, N, \quad k = 0, 1, \dots$$

where m is a counter that indicates the m^{th} servo sector at the specific track used for track following and N is the number of servo sectors. Using the notation e^m to indicate PES $e(t)$ for $t = (m+kN)\Delta\tau$, the time dependent PES $e(t)$ is written as

$$e^m = e(t), \quad t = (m+kN) \cdot \Delta\tau$$

If the servo sectors are equally spaced and the rotational speed of the HDD is constant, the PES sampling interval $\Delta\tau = \frac{v}{60}N$, where v is the rotational speed of the disk. To model the effect of timing jitter on PES e^m , variations in the PES sampling interval $\Delta\tau$ will be considered as one of the quality measures for the PES.

The most commonly used servo pattern is the (quadrature) amplitude servo pattern, shown in Figure 1. Independent servo burst represented by the magnetized fields A and B in Figure 1 are used to generate a readback signal $R(t)$.

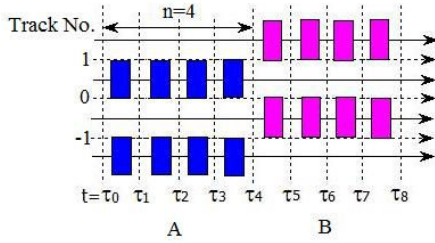


Fig. 1. Amplitude servo pattern.

Let the readback signals generated from A and B bursts at the m^{th} servo sector be $R_A^m(t)$ and $R_B^m(t)$ respectively:

$$\begin{aligned} R_A^m(t) &= R^m(t) \quad \tau_0 < t < \tau_n \\ R_B^m(t) &= R^m(t) \quad \tau_n < t < \tau_{2n} \end{aligned}$$

and

$$\begin{aligned} \bar{R}_{A_i}^m &= \max_{\tau_{i-1} < t < \tau_i} R_A^m(t), \quad i = 1, \dots, n \\ \bar{R}_{B_i}^m &= \max_{\tau_{n+i-1} < t < \tau_{n+i}} R_B^m(t), \quad i = 1, \dots, n \end{aligned}$$

where $R^m(t)$ is the readback signal generated from m^{th} servo sector, n is the number of pulse in either A burst or B burst and m is the counter of servo sectors. The amplitudes of the readback signals generated from the A and B bursts vary with the position of the read head. The difference between the amplitudes of $R_A^m(t)$ and $R_B^m(t)$ is used to decode PES e^m as in [1] via

$$e^m = \sum_{i=0}^n \bar{R}_{A_i}^m - \bar{R}_{B_i}^m$$

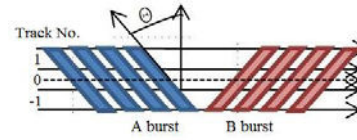
The amplitude servo pattern generates nonlinear responses to head positions due to MR heads' inherent nonlinearity [5]. Timing-based servo patterns are not directly effected by MR head response and for that purpose chevron and differential frequency servo patterns will be considered [16]. As shown in Figure 2, slanted parallel magnetic strips are located along the track in reflection symmetry with respect to a line perpendicular to the track. Several strips are used

to allow for time averaging. Many studies have been carried out on the chevron servo pattern [7], [10], [13], [12], [14] illustrating the favorable properties on the (linearity) of the PES.

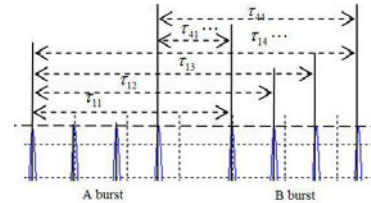
Each pulse generated from a transition in a magnetic strip will be spatially aligned proportional to the amount of time between the strips, indicating the timing-based nature of the chevron pattern. The relative time difference between these pulses is used to decode PES e^m as in [14] via

$$e^m = \sum_{p=1}^n \tau_{1p}^m + \sum_{p=1}^n \tau_{2p}^m + \dots + \sum_{p=1}^n \tau_{np}^m - \bar{e}$$

where τ_{ij} indicates the time from the i^{th} pattern in A burst to the j^{th} pattern in B burst, as illustrated in Figure 2-(b). In addition \bar{e} is the known time difference in case we were exactly at the middle of the pattern, indicated by dotted line in Figure 2-(a).



(a) Chevron servo pattern.



(b) Readback signal demodulation.

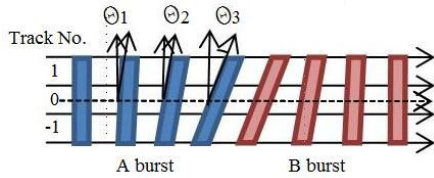
Fig. 2. (a) Chevron servo pattern. (b) Readback signal demodulation for the chevron servo pattern. τ_{ij} indicates the time from the i^{th} pattern in A burst to the j^{th} pattern in B burst.

Another timing-based servo pattern investigated in this paper is the differential frequency pattern and depicted in Figure 3 [16]. This servo pattern also contains two separate burst groups, but they are oriented in a rotational symmetry with respect to a center point on the data track. Again several strips are used to allow for time averaging.

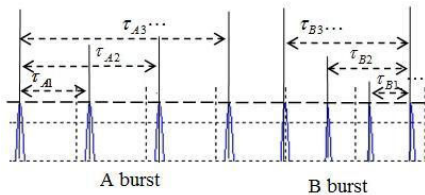
As with the chevron servo pattern, each pulse generated from a magnetic strip will be spatially aligned proportional to the amount of time between the strips [16]. The relative time between these pulses is used to decode PES e^m via

$$\begin{aligned} T_A^m &= \sum_{p=1}^{2(n-1)} \tau_{A_i}^m \\ T_B^m &= \sum_{p=1}^{2(n-1)} \tau_{B_i}^m \\ e^m &= T_A^m - T_B^m \end{aligned}$$

where τ_{Ai} indicates the time from the first bar in A burst to the rest of bars and τ_{Bi} indicates the time from the last bar in B burst to the rest of bars.



(a) Differential frequency pattern.



(b) Readback signal demodulation.

Fig. 3. (a) Differential frequency pattern. (b) Readback signal demodulation for the differential frequency pattern. τ_{Ai} indicates the time from the first bar in A burst to the rest of bars and τ_{Bi} indicates the time from the last bar in B burst to the rest of bars.

B. Quality measures for PES

In addition to the readback signal quality factors addressed in Section II-B, there are servo related factors that influence PES quality. Depending on which servo patterns are used, MR heads' inherent nonlinearity causes nonlinearity in PES, thereby degrading PES quality [5]. The PES quality is also affected by the timing-jitter in the PES sampling interval $\Delta\tau$ caused by variations in servo sector locations due manufacturing and HDD rotational speed tolerances. A dispersion parameter δ is used to model timing jitter by specifying the dispersion of the PES data (servo sectors) distributed on a disk. The dispersion parameter δ is defined as

$$\sigma^2 = \left(\frac{2\pi\delta}{N}\right)^2 \quad (4)$$

where σ^2 is the variance of PES data position distribution and N is the number of servo sectors. Using the notation $\aleph(\mu, \lambda)$ as detailed above, we model the PES corrupted by timing jitter \tilde{e}^m as

$$\tilde{e}^m = e(t), \quad \text{for } t = (m + kN) \cdot \Delta\tau$$

where the PES sampling interval $\Delta\tau \sim \aleph\left(\frac{v}{60}N, \delta\right)$ and v is the speed of a disk. Detailed simulation results of the timing jitter effect will be presented in Section IV.

C. HDD case study

In a session of a technical meeting of IEE Japan, a HDD benchmark [15] was presented for track-following control of HDD model at a track density of 100kTPI. In the benchmark,

torque disturbance, flutter disturbance, repeatable runout (RRO), and sensor noise are considered. Since the goal is to predict PES quality and servo pattern performance for future product planning, the data of Japanese HDD benchmark is extrapolated to a track density of 400kTPI in the simulation study of this paper and summarized in Table I. In our extrapolation of HDD parameters, the track density and spindle speed have been increased and the track width decreased to achieve 400kTPI. Based on these changes, the dynamics of the plant, periodic and non-periodic disturbances and the servo controller were modified to provide a realistic simulation study [18].

TABLE I
HDD PARAMETERS AT 400kTPI.

Parameters	Values	Units
Track density	400	[kTPI]
Track width	63.5	[nm]
Spindle speed	15,000	[rpm]

IV. OVERVIEW OF SIMULATION RESULTS

A. Simulation results

A simulation has been carried out for the 400kTPI HDD case study to evaluate PES quality and servo pattern performance when varying the different quality measures of the amplitude, chevron and differential frequency patterns. The resulting PES, without considering any effect of the quality factors discussed in Section II and Section III, is shown in Figure 4 as function of the 220 servo sector used in the HDD benchmark.

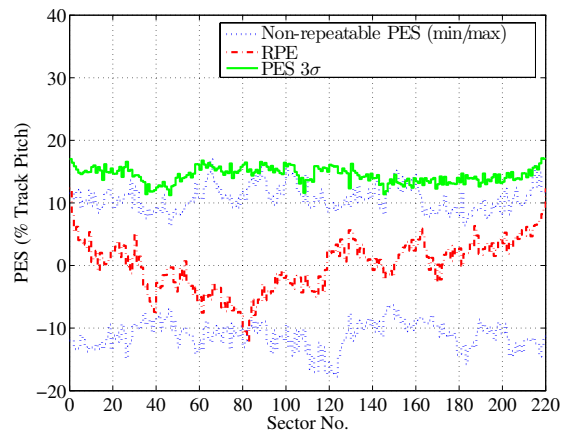


Fig. 4. PES at a track density of 400kTPI without considering the effect of the quality factors discussed in Section II and Section III. The green solid line is the 3σ value of the PES, the red dashed line is repeatable position error, and the blue dotted lines are non-repeatable position errors (min/max) over the 220 HDD servo sectors.

A distinction is made between the effects of repeatable and non-repeatable position errors on the PES in Figure 4. From the closed-loop servo track following simulation results, the 3σ value of the PES is a good indication of *servo performance*. Running the simulation for multiple revolutions

of the HDD allows the computation of the PES 3σ value, including the non-repeatable error. It can be seen in Figure 4 that the 3σ value of the PES is obtained at around 15% of a track pitch without considering the effect of quality factors.

B. Servo performance for different servo patterns

In order to provide simulation results that investigates the sensitivity of the servo performance as a function of the servo patterns, the quality factors of the readback signal $R(t)$ discussed in Section II and the quality factors on the PES signal discussed in Section III must be included. As mentioned in Section II, amplitude fluctuation noise, transition jitter and readback signal sampling are the main quality factors to be considered in the readback signal.

Amplitude fluctuations due to media noise in the readback signal was modeled by white noise on the bit pattern signal $b(k)$ with the variance parameter λ_η and given in (1). The sensitivity of each servo pattern to these amplitude fluctuation noise is shown in Figure 5.

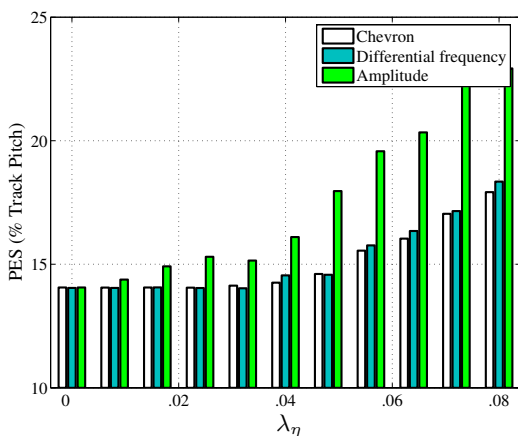


Fig. 5. Servo performance measured by 3σ of the PES as a function of readback amplitude fluctuation noise effects in (1), where λ_η is the variance of the amplitude fluctuation noise distribution.

It can be observed from Figure 5 that amplitude fluctuation noise causes degradation of servo performance for the amplitude-based servo pattern. As expected, the servo performance is less sensitive to readback amplitude fluctuation noise for the timing-based servo patterns (chevron and differential frequency). On the other hand, timing variations caused by transition jitter in the servo patterns will influence servo performance for the timing-based servo patterns as indicated in Figure 6. Transition jitter was modeled by white noise time shift in the transition response $h(k, w)$ with the variance parameter λ_γ and given in (2).

It can be observed from Figure 6 that both the chevron and differential frequency timing-based servo patterns are sensitive to transition jitter. However, the differential frequency servo pattern is less sensitive to transition noise than the chevron pattern, since each magnetic bar in the chevron servo pattern is placed closer to neighboring bars than each magnetic bar in the differential frequency. Obviously, the effect of timing jitter in the readback signal can be eliminated

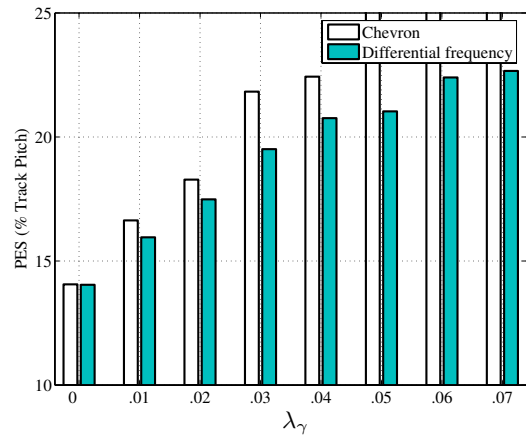


Fig. 6. Servo performance measured by 3σ of the PES as a function of transition jitter effects in (2), where λ_γ is the variance of transition jitter distribution. The unshaded and shaded bars indicate the PES generated from the chevron and differential frequency servo patterns respectively.

when using a BPM with precise servo patterns, motivating the use of BPM for servo sections.

Next to timing jitter, sampling effects of the readback signal greatly affects the signal quality in timing-based servo patterns. The effect of readback signal sampling on servo performance measured can be studied by changing the number of samples N_p used to sample the bit pattern signal $b(k)$ and given in (3). The sensitivity of each servo pattern to readback signal sampling is shown in Figure 7. Again it can be observed that the differential frequency pattern is less sensitive than the chevron pattern to readback signal sampling variations.

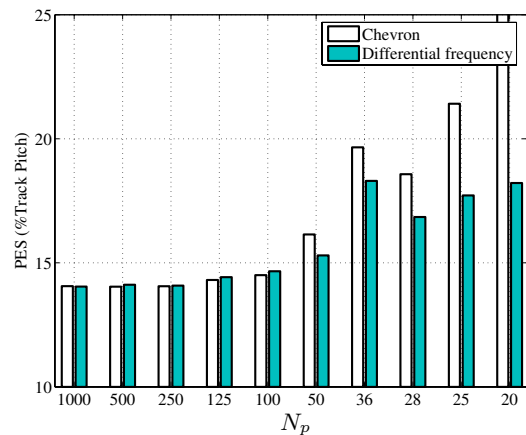


Fig. 7. Servo performance measured by 3σ of the PES as a function of readback signal sampling, where N_p is the number of samples used to sample the bit pattern signal $b(k)$ modeled in (3). The unshaded and shaded bars indicate the PES generated from the chevron and differential frequency servo patterns respectively.

Next to the relative spacing of the bars in the timing-based servo patterns used for averaging, there is another main difference between the chevron and the differential frequency pattern that explains the superior results of the differential frequency pattern. The main difference lies is the

asymmetry in timing difference when going off-track in positive or and negative direction. The rotational symmetry of the differential pattern provides time difference signals that are identical, but appearing at different absolute times. The chevron pattern provides time difference signals that became smaller or larger, depending on the off-track direction. As illustrated by the simulations, the symmetric timing difference in the rotational symmetry of the differential pattern allows better time averaging of spatial (readback signal noise) and readback sampling effects, concluding that the differential frequency pattern can outperform the chevron pattern with respect to PES quality and resulting servo performance.

As a final comparison, the timing jitter effect of the PES due variations in spatial location of servo sectors or variations in rotational speed of the HDD is depicted in Figure 8. Timing jitter effects in the PES are independent of the actual servo sector patterns. It is clear that servo performance degrades as the dispersion parameter δ in (4) increases, as variations in the PES sampling interval $\Delta\tau$ increases.

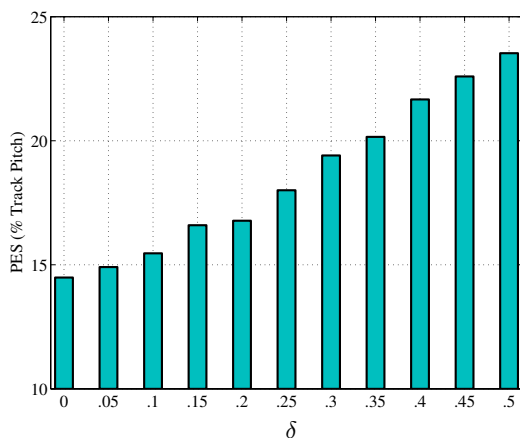


Fig. 8. Servo performance measured by 3σ of the PES as a function of the (spatial) dispersion parameter δ in (4) and is independent of the servo patterns used.

V. SUMMARY AND CONCLUSIONS

Servo performance measured by the 3σ value of a Position Error Signal (PES) in the closed-loop control of a HDD actuator is modeled as a function of quality factors on the readback signal that include amplitude fluctuation noise, transition jitter and readback signal sampling. In addition, timing jitter effects in the PES due to spatial variations in servo sectors was taking into account to study servo performance. The quality factors on the readback signal were evaluated for a conventional amplitude based servo pattern and a chevron pattern, and differential frequency pattern that are both timing-based servo patterns. To draw conclusions on the performance of the different servo patterns, a 400kTPI benchmark was used to compute the 3σ value of the PES with a dedicated magnetic readback signal simulation and signal decoding along with a closed-loop simulation.

For the timing-based servo patterns, readback signal sampling and transition jitter were found to affect PES quality,

but the effect on the differential frequency pattern is significantly less due to improved relative spacing of the magnetic islands within the pattern and the favorable rotational symmetry that allows for better averaging when going off-track in either positive or negative direction. In addition, when creating BPM servo patterns on a disk repeatedly, the differential frequency pattern has an advantage in providing alignment due to the rotational symmetry. Future work on investigating the effect of position and shape variation of patterned bits is required for better servo pattern performance evaluation and guiding fabrication process.

VI. ACKNOWLEDGEMENTS

This research was supported by a grant from the EHDR Information Storage Industry Consortium (INSIC). The authors gratefully acknowledge the support.

REFERENCES

- [1] A. Mamun, G. Guo, and C. Bi, *Hard Disk Drive: Mechatronics and Control*. Boca Raton, FL: CRC Press, 2007.
- [2] R. Sbiaa and S. Piramanayagam, "Patterned media towards nano-bit magnetic recording: Fabrication and challenges," *Recent Patents on Nanotechnology*, vol. 1, pp. 29–40, 2007.
- [3] A. Barany and H. Bertram, "Transition position and amplitude fluctuation noise model for longitudinal thin film media," *IEEE Trans. on Magnetics*, vol. 23, pp. 2374–2376, 1987.
- [4] Y. T. C. Tsang, "Disk-noise induced peak jitters in high density recording," *IEEE Trans. on Magnetics*, vol. 29, pp. 3975–3977, 1993.
- [5] A. Sacks and W. Messner, "MR head effects on PES generation: Simulation and experiment," *IEEE Trans. on Magnetics*, vol. 32, pp. 1773–1778, 1996.
- [6] K. Akagi, K. Yasuna, and K. Shishida, "Optimizing servo-signal design for a hard-disk drives," *Microsystem Technologies*, vol. 11, pp. 784–789, 2005.
- [7] J. Zhu, X. Lin, L. Guan, and W. Messner, "Recording, noise, and servo characteristics of patterned thin film media," *IEEE Trans. on Magnetics*, vol. 36, pp. 23–29, 2000.
- [8] A. Kikitsu, Y. Kamata, M. Sakurai, and K. Naito, "Recent progress of patterned media," *IEEE Trans. on Magnetics*, vol. 43, pp. 3685–3688, 2007.
- [9] H. Richter, A. Dobin, O. Heinonen, K. Gao, R. V.D. Veerdonk, R. Lynch, J. Xue, D. Weller, P. Asselin, M. Erden, and R. Brockie, "Recording on bit-patterned media at densities of 1 Tb/in² and beyond," *IEEE Trans. on Magnetics*, vol. 42, pp. 2255–2260, 2006.
- [10] M. Moneck, J. Zhu, Y. Tang, K. Moon, H. Lee, S. Zhang, X. Che, and N. Takahashi, "Lithographically patterned servo position error signal patterns in perpendicular disks," *Journal of Applied Physics*, vol. 103, pp. 07C511–07C511–3, 2008.
- [11] O. Heinonen and K. Gao, "Extensions of perpendicular recording," *Journal of Magnetism and Magnetic Materials*, vol. 320, pp. 2885–2888, 2008.
- [12] X. Lin, J. Zhu, and W. Messner, "Investigation of advanced position error signal patterns in patterned media," *Journal of Applied Physics*, vol. 87, pp. 5117–5119, 2000.
- [13] E. Hughes and W. Messner, "New servo pattern for hard disk storage using pattern media," *Journal of Applied Physics*, vol. 93, pp. 7002–7004, 2003.
- [14] E. Hughes and W. Messner, "Characterization of three servo patterns for position error signal generation in hard drives," in *Proc. American Control Conference*, (Denver, CO), pp. 4317–4321, 2003.
- [15] "Japan HDD benchmark problem." <http://mizugaki.iis.u-tokyo.ac.jp/nssl/>.
- [16] W. Messner, J. Zhu, and X. Lin, "Frequency modulation pattern for disk drive assemblies," Tech. Rep. US 6,754,016 B2, United States Patent, 2004.
- [17] B. Bane Vasic and E. Kurtas, *Coding and Signal Processing for Magnetic Recording Systems*. Boca Raton, FL: CRC Press, 2005.
- [18] Y. Han and R. de Callafon, "Evaluation of track following servo performance of high density hard disk drives using patterned media," *To appear in IEEE Trans. on Magnetics*, 2009.